INTERNATIONAL JOURNAL OF
NUMERICAL ANALYSIS AND MODELING
Volume 11, Number 2, Pages 358–371

INTERIOR LAYERS IN A SINGULARLY PERTURBED TIME DEPENDENT CONVECTION–DIFFUSION PROBLEM

J.L. GRACIA AND E. O'RIORDAN*

(Communicated by C. Rodrigo)

This paper is dedicated to Francisco Lisbona, on the occasion of his 65th birthday

Abstract. A linear singularly perturbed time dependent convection–diffusion problem is examined. The initial condition is designed to have steep gradients in the vicinity of the inflow point, which are transported in time, thus creating a moving interior shock layer. The location of this interior layer is tracked by the characteristics of the reduced first order problem. A numerical method is designed and analysed, which consists of a monotone finite difference operator and a piecewise-uniform Shishkin mesh, which is aligned to the characteristic curve emanating from the initial shock location. Parameter explicit error bounds are established and numerical results are presented to illustrate the performance of the numerical method.

Key words. Singular perturbation, interior layer, Shishkin mesh.

1. Introduction

Standard numerical algorithms for partial differential equations are inefficient when steep gradients are present in the solution. Steep gradients arise naturally in the solutions of singularly perturbed problems and in problems where the data (coefficients, source term, boundary/initial conditions, boundary of the domain) are not smooth. Problems with incompatibilities between the initial and boundary data in parabolic problems arise, for example, in mathematical models in poroelasticity [4]. In particular, interior layers can appear, in the solution of a singularly perturbed convection-diffusion parabolic problem, throughout the entire domain if the initial function and the boundary condition do not coincide at the inflow corner point. An alternative mathematical model could be considered where such an incompatibility is regularized by an initial function which is itself the solution of a singularly perturbed ordinary differential equation. In this paper, we construct and analyse a numerical method for a class of singularly perturbed convection–diffusion parabolic problems, where the solution has steep gradients both internally and in a small neighbourhood of the inflow corner point.

This paper is a companion paper to [5], where the following class of problems was studied: Find $\hat{u}$ that satisfies the singularly perturbed differential equation

$$\text{(1a)}\quad \hat{L}_\varepsilon \hat{u} := -\varepsilon \hat{u}_{ss} + \hat{a}(t)\hat{u}_s + \hat{u}_t = \hat{f}(s,t), \quad (s,t) \in Q := (0,1)\times(0,T],$$

$$\text{(1b)}\quad \hat{a}(t) \geq \alpha > 0, t \geq 0;$$

and the boundary and initial conditions

$$\text{(1c)}\quad \hat{u}(0,t) = \hat{\phi}_L(t),\ \hat{u}(1,t) = \hat{\phi}_R(t), \quad 0 < t \leq T,$$

$$\text{(1d)}\quad \hat{u}(s,0) = \hat{\phi}(s;\varepsilon), \quad 0 \leq s \leq 1.$$

Received by the editors October 17, 2012 and, in revised form, June 12, 2013.
2000 *Mathematics Subject Classification.* 65L11,65L12.
*Corresponding author.

The initial condition $\hat{\phi}$ is smooth, but contains an interior layer (see (3)) in the vicinity of a point $s = d, 0 < d < 1$, with d independent of ε. The characteristic curve associated with the reduced differential equation (formally set $\varepsilon = 0$ in (1)) can be described by the set of points

$$\Gamma^* := \{(\gamma(t), t) |\, \gamma'(t) = \hat{a}(t),\ 0 < \gamma(0) = d < 1\}, \tag{2a}$$

that partitions the domain $\bar{Q}$ into two subdomains either side of Γ^*

$$\bar{Q}^- := \{(s, t) |\, s \le \gamma(t) \le 1,\ 0 \le t \le T\}, \tag{2b}$$

$$\bar{Q}^+ := \{(s, t) |\, s \ge \gamma(t) \ge 0,\ 0 \le t \le T\}. \tag{2c}$$

The solution of problem (1) will have an interior layer of width $O(\sqrt{\varepsilon})$ (emanating from the initial condition) which moves in time along Γ^*. In general a boundary layer of width $O(\varepsilon)$ will also appear in the vicinity of the edge $x = 1$. We restrict the size of the final time T so that the interior layer does not interact with this boundary layer. Since $\hat{a} > 0$, the function $\gamma(t)$ is monotonically increasing. Thus, we limit the final time T such that $0 < c < 1 - \gamma(T)$. The parabolic problem examined in [5] may be viewed as a regularization of a singularly perturbed parabolic problem with a discontinuous initial condition.

In this paper, we consider the effect of an interior layer forming initially within a distance greater than or equal to $C\varepsilon^p$, with $p < 1/2$, of the corner $(0, 0)$. The main differences between this paper and [5] occur to the left (in the subdomain $\bar{Q}^-$) of the interior layer. On the right side of the interior layer (in the subdomain $\bar{Q}^+$), the numerical method is essentially identical to what was reported in [5]. Both the numerical method and its associated numerical analysis are different in $\bar{Q}^-$ to what was presented in [5]. The parabolic problem examined in this paper may be viewed as a regularization of a singularly perturbed parabolic problem where the inflow boundary condition and the initial condition do not agree at the inflow corner. Although the solution of the regularized problem does not approximate the solution of a problem with an incompatibility in the vicinity of the inflow corner point $(0, 0)$, the regularized problem may be of interest to researchers interested in simulating the creation of a travelling interior layer, such as can be seen in Figure 3 in §5.2.

In this paper, the time derivatives of the interior layer component (denoted here by $\hat{z}^-$) depend adversely on d, which in turn depends on ε. To construct a parameter-uniform numerical method, the region $\bar{Q}^-$ is further decomposed into two subregions. The first subregion of $\bar{Q}^-$ is designed so that a fine mesh is aligned to the characteristic curve Γ^*. The second subregion is what remains in $\bar{Q}^-$ after this first subregion has been identified. Within each subregion, a particular coordinate system is utilized so that the discretization within each subregion takes place on a rectangular mesh.

In §2, the solution of the continuous problem is decomposed into a sum of components and parameter explicit bounds on each of these components are established. A coordinate transformation, related to the characteristic curve Γ^*, is introduced and the time derivatives of the interior layer component are shown to be bounded in this transformed coordinate system. In §3, the discrete problem is constructed, which involves a piecewise-uniform Shishkin mesh. The numerical method is analysed in §4 and some numerical results are presented in §5.1 to illustrate the theoretical error bounds.

The theoretical analysis in this paper requires that the location of the interior layer in the initial condition is bounded away from the corner $(0, 0)$ by a distance $d > C\sqrt{\varepsilon}$. In §5.2, we present numerical results for the numerical method presented

in [5] in the case where $0 < d \leq C\sqrt{\varepsilon}$. These experimental results suggest that the numerical method from [5] is globally pointwise accurate, although the proof of the uniform convergence of the numerical method remains an open question.

Throughout the paper, C denotes a generic constant that is independent of the singular perturbation parameter ε and of all discretization parameters. We denote by $\|\cdot\|_{\bar{D}}$ the maximum norm over any region D, which is defined by $\|g\|_{\bar{D}} := \max_{x\in\bar{D}} |g(x)|$ for any function g. The space $\mathcal{C}^{n+\lambda}(D)$, where $D \subset \mathbf{R}^2$ denotes an open set, is defined by

$$\mathcal{C}^{n+\lambda}(D) := \{z : \frac{\partial^{i+j} z}{\partial x^i \partial y^j} \in \mathcal{C}^{0+\lambda}(D),\ 0 \leq i+2j \leq n\},$$

where $\mathcal{C}^{0+\lambda}(D)$ is the set of all functions that are Hölder continuous of degree λ.

2. Continuous problem

In this paper, we examine the singularly perturbed differential equation (1a) with the boundary conditions (1c) and an initial condition, which for sufficiently regular and compatible data (see [5] for a detailed discussion), ensures that $\hat{u} \in C^{4+\lambda}(\bar{Q})$. However, the initial condition is assumed to contain an interior layer to the right of a point $d = \varepsilon^p$, with $p < 1/2$. We consider initial conditions of the form

$$\hat{u}(s,0) := \begin{cases} 0, & \text{if } 0 \leq s \leq d, \\ \hat{\phi}_v + \hat{\phi}_w, & \text{if } d \leq s \leq 1, \end{cases} \tag{3a}$$

where for $0 \leq k \leq 4$,

$$|\hat{\phi}_v(s)|_k \leq C, \quad |\hat{\phi}_w(s)|_k \leq C\varepsilon^{-k/2} e^{-\frac{s-d}{\sqrt{\varepsilon}}}, \quad s \in [d,1]. \tag{3b}$$

In particular, the left boundary condition satisfies $\hat{\phi}_L(0) = \hat{\phi}'_L(0) = \hat{\phi}''_L(0) = 0$ at the corner $(0,0)$.

The differential operator associated with problem (1) satisfies a maximum principle. Hence, we have the stability bound

$$\|\hat{u}\|_{\bar{Q}} \leq C. \tag{4}$$

Lemma 1. [5] *There exist functions $\hat{r}_0(t)$, $\hat{r}_1(t)$, and $\hat{r}_2(t)$ such that the solutions $\hat{v}^-$, and $\hat{v}^+$ of the problems*

$$\hat{L}_\varepsilon \hat{v}^\pm := -\varepsilon \hat{v}^\pm_{ss} + \hat{a}(t)\hat{v}^\pm_s + \hat{v}^\pm_t = \hat{f}(s,t), \quad (s,t) \in Q^\pm,$$
$$\hat{v}^-(s,0) = 0,\ 0 \leq s \leq d,\ \hat{v}^-(0,t) = \hat{\phi}_L(t),\ \hat{v}^-(\gamma(t),t) = \hat{r}_0(t),\ 0 < t \leq T,$$
$$\hat{v}^+(s,0) = \hat{\phi}_v(s),\ d \leq s \leq 1,\ \hat{v}^+(\gamma(t),t) = \hat{r}_1(t),\ \hat{v}^+(1,t) = \hat{r}_2(t),\ 0 < t \leq T,$$

satisfy the bounds

$$\Big\| \frac{\partial^{j+m} \hat{v}^\pm}{\partial s^j \partial t^m} \Big\|_{\bar{Q}^\pm} \leq C(1 + \varepsilon^{2-(j+m)}), \quad 0 \leq j+2m \leq 4. \tag{5}$$

On the region $\bar{Q}^-$, the interior layer component $\hat{z}^- = \hat{u} - \hat{v}^-$ satisfies

$$\hat{L}_\varepsilon \hat{z}^- = 0, \quad (s,t) \in Q^-, \quad \hat{z}^-(s,0) = 0, \quad 0 \leq s \leq d, \tag{6a}$$
$$\hat{z}^-(0,t) = 0,\ \hat{z}^-(\gamma(t),t) = (\hat{u} - \hat{v}^-)(\gamma(t),t), \quad 0 \leq t \leq T. \tag{6b}$$

Lemma 2. *The solution of (6) satisfies the pointwise bound*

$$|\hat{z}^-(s,t)| \leq Ce^{-\sqrt{\frac{\alpha}{\varepsilon}}(\gamma(t)-s)}. \tag{7}$$

In the subregion

$$S := \{(s,t) \in \bar{Q}^- \,|\, \gamma(t) - d + \mu \leq s \leq \gamma(t),\ \text{and } 0 \leq t \leq T\}, \tag{8}$$

where $\mu = O(\sqrt{\varepsilon})$, the derivatives of the component $\hat{z}^-$ satisfy

$$\left\| \frac{\partial^j \hat{z}^-}{\partial s^j} \right\|_S \le C\varepsilon^{-j/2},\ 1 \le j \le 4, \quad \left\| \frac{\partial^m \hat{z}^-}{\partial t^m} \right\|_S \le C\varepsilon^{-m/2},\ m = 1, 2. \tag{9}$$

Proof. Note that $\hat{z}^-(s,0) = 0$, $\hat{z}^-(0,t) = 0$, and with the bounds (5), $|\hat{z}(\gamma(t),t)| \le C$. For the interior points of $\bar{Q}^-$ we have that

$$\hat{L}_\varepsilon \big(e^{\alpha t} e^{-\sqrt{\frac{\alpha}{\varepsilon}}(\gamma(t)-s)} \big) = 0.$$

The bound (7) follows from the maximum principle.

To deduce bounds on the derivatives of $\hat{z}^-$, we introduce the following change of variable

$$\eta := \frac{s + d - \gamma(t)}{\sqrt{\varepsilon}},\ \tau_1 := t; \qquad \check{z}^-(\eta, \tau_1) := \hat{z}^-(s,t). \tag{10}$$

By the chain rule

$$\frac{\partial^j \hat{z}^-}{\partial s^j} = \varepsilon^{-j/2} \frac{\partial^j \check{z}^-}{\partial \eta^j},\ 1 \le j \le 4, \quad \frac{\partial \hat{z}^-}{\partial t} = -\frac{\check{a}(\tau_1)}{\sqrt{\varepsilon}} \frac{\partial \check{z}^-}{\partial \eta} + \frac{\partial \check{z}^-}{\partial \tau_1}. \tag{11}$$

In this coordinate system, the function $\check{z}^-(\eta, \tau_1)$ satisfies the heat equation

$$\check{z}^-_{\tau_1} - \check{z}^-_{\eta\eta} = 0,$$

and we can apply the classical theory (see, for example, [1] or [2]) to this equation in a rectangular region $(\eta, \tau_1) \in \check{S} := (\mu/\sqrt{\varepsilon}, d/\sqrt{\varepsilon}) \times (0, T]$. Note that we need to impose $d \ge C\sqrt{\varepsilon}$ in order that the width of the transformed domain has a lower bound which is ε–independent and $\mu = O(\sqrt{\varepsilon})$ so that the region $\check{S}$ is a fixed $O(1)$ distance from the corner $(0,0)$.

Recall that, $\check{z}^-(\eta, 0) = 0$. On the two edges $\eta = \mu/\sqrt{\varepsilon}$ and $\eta = d/\sqrt{\varepsilon}$ we use the decomposition $\hat{z}^- = \hat{u} - \hat{v}^-$. Bounds for the components $\hat{u}$, $\hat{v}^-$ on these two edges are deduced as follows: First, from (5), the transformed regular component $\check{v}^-(\eta, \tau_1) := \hat{v}^-(s,t)$ satisfies

$$\left| \frac{\partial^m \check{v}^-}{\partial \tau_1^m}(p/\sqrt{\varepsilon}, \tau_1) \right| \le C,\ p = \mu, d; \quad m = 1, 2.$$

Secondly, $\check{u}(\eta, \tau_1) := \hat{u}(s,t)$ also satisfies the heat equation $\check{u}_{\tau_1} - \check{u}_{\eta\eta} = \check{f}$ in the new variables. Note that

$$\left| \frac{\partial^i \check{u}}{\partial \eta^i}(\eta, 0) \right| \le C, \quad i = 1, 2, 3, 4.$$

On the edges $\eta = \mu/\sqrt{\varepsilon}, d/\sqrt{\varepsilon}$, interior (to the entire domain Q) local Schauder point estimates yield

$$\left| \frac{\partial^m \check{u}}{\partial \tau_1^m}(p/\sqrt{\varepsilon}, \tau_1) \right| \le C,\ p = \mu, d; \quad m = 1, 2.$$

Therefore,

$$\left| \frac{\partial^m \check{z}^-}{\partial \tau_1^m}(p/\sqrt{\varepsilon}, \tau_1) \right| \le C,\ p = \mu, d; \quad m = 1, 2.$$

From the previous estimates, we deduce that

$$\left| \frac{\partial^{j+m} \check{z}^-}{\partial \eta^j \partial \tau_1^m}(\eta, \tau_1) \right| \le C, \quad 1 \le j + 2m \le 4,\ (\eta, \tau_1) \in \check{S}. \tag{12}$$

The bounds in (9) follow from (11), (12) and the fact that

$$\frac{\partial^2 \hat{z}^-}{\partial t^2} = \frac{\partial^2 \check{z}^-}{\partial \eta^2} \left(\frac{\partial \eta}{\partial t} \right)^2 + 2 \frac{\partial^2 z^-}{\partial \eta \partial \tau_1} \frac{\partial \eta}{\partial t} + \frac{\partial \check{z}^-}{\partial \eta} \frac{\partial^2 \eta}{\partial t^2} + \frac{\partial^2 \check{z}^-}{\partial \tau_1^2}.$$

□

Note that the bounds on the time derivatives of the component $\hat{z}^-$ depend adversely on the singular perturbation parameter and the coordinate system (s,t) is not aligned with the characteristic curve Γ^*. Nevertheless, we do note from (11) that the directional derivative along the characteristic curve satisfies

$$\left|(\hat{a}\hat{z}^-_s + \hat{z}^-_t)\right| \leq C, \quad (s,t) \in \bar{Q}^-. \tag{13}$$

From the bounds (12), we also note that in the subregion S, defined in (8),

$$\left|\frac{\partial^j \tilde{z}^-}{\partial \varsigma^j}\right| \leq C\varepsilon^{-j/2}, \quad 0 \leq j \leq 4, \quad \left|\frac{\partial^m \tilde{z}^-}{\partial \tau_2^m}\right| \leq C, \quad m = 1,2$$

where $\varsigma := s - \gamma(t) + d,\ \tau_2 := t$; and $\tilde{z}^-(\varsigma,\tau_2) := \hat{z}^-(s,t)$.

Motivated by these parameter independent bounds on the time derivatives, we consider the following mapping $X : (s,t) \to (x,\tau)$, defined by $\tau := t$ and

$$x := \begin{cases} s - \gamma(t) + d, & \text{if } (s,t) \in Q_2^-, \\ \dfrac{d-\sigma_1}{\gamma(t)-\sigma_1}s, & \text{if } (s,t) \in Q_1^- := Q^- \setminus Q_2^-, \\ 1 - \dfrac{1-d}{1-\gamma(t)}(1-s), & \text{if } (s,t) \in Q^+, \end{cases}$$

$$Q_2^- := \{(s,t)\,|\,\gamma(t) - \sigma_1 < s < \gamma(t),\ t \in (0,T]\},$$

where $0 < \sigma_1 \leq 0.25d$ is specified below. The transformed subregions are denoted by $\Omega^+ := X(Q^+)$, $\Omega_1^- := X(Q_1^-)$, and $\Omega_2^- := X(Q_2^-)$, respectively. We adopt the following notation throughout the remainder of the paper

$$u(x,\tau) := \hat{u}(s,t).$$

The mapping is not smooth along the interfaces $\bar{Q}^+ \cap \bar{Q}_2^-$ and $\bar{Q}_1^- \cap \bar{Q}_2^-$; and note that $\hat{u} \in C^{4+\lambda}(\bar{Q})$, but $u \notin C^{1+\lambda}(\bar{\Omega})$.

Using this map, problem (1) transforms into

$$(-\varepsilon g^2 u_{xx} + \kappa u_x + u_\tau)(x,\tau) = f(x,\tau); \quad (x,\tau) \in \Omega, \tag{14a}$$

$$[u](x,\tau) = 0,\ -\varepsilon[g u_x](x,\tau) = 0, \quad x = d - \sigma_1, d,\ \tau > 0, \tag{14b}$$

$$u(x,\tau) = \hat{u}(s,t), \quad (x,\tau) \in \partial\Omega, \tag{14c}$$

$$\Omega := \Omega_1^- \cup \Omega_2^- \cup \Omega^+, \quad \partial\Omega = \bar{\Omega}\backslash(0,1) \times (0,T],$$

with $[g u_x](x,\tau) := g(x^+,\tau)u_x(x^+,\tau) - g(x^-,\tau)u_x(x^-,\tau)$. The coefficients g, κ are

$$\kappa(x,\tau) := \begin{cases} \dfrac{a(\tau)(d-\sigma_1)}{\gamma(\tau)-\sigma_1}\big(1 - \dfrac{x}{d-\sigma_1}\big), & \text{in } \Omega_1^-, \\ 0, & \text{in } \Omega_2^-, \\ \dfrac{a(\tau)(1-d)}{1-\gamma(\tau)}\big(1 - \dfrac{1-x}{1-d}\big), & \text{in } \Omega^+, \end{cases} \tag{14d}$$

$$g(x,\tau) := \begin{cases} \dfrac{d-\sigma_1}{\gamma(\tau)-\sigma_1}, & \text{in } \Omega_1^-, \\ 1, & \text{in } \Omega_2^-, \\ \dfrac{1-d}{1-\gamma(\tau)}, & \text{in } \Omega^+. \end{cases} \tag{14e}$$

Observe that $\varepsilon[gu_x](x,\tau) = \varepsilon[\hat{u}_s](s,\tau)$, $(s,\tau) \in \bar{Q}_1^- \cap \bar{Q}_2^-$. Initial estimates of the solution u in these new variables (x,τ) are deduced as follows. Note that

$$\frac{\partial^j u}{\partial x^j} = \frac{\partial^j \hat{u}}{\partial s^j}\Big(\frac{\partial s}{\partial x}\Big)^j,\ 1 \le j \le 4, \quad \frac{\partial u}{\partial \tau} = \frac{\partial \hat{u}}{\partial s}\frac{\partial s}{\partial \tau} + \frac{\partial \hat{u}}{\partial t},$$
$$\frac{\partial^2 u}{\partial \tau^2} = \frac{\partial^2 \hat{u}}{\partial s^2}\left(\frac{\partial s}{\partial \tau}\right)^2 + 2\frac{\partial^2 \hat{u}}{\partial s \partial t}\frac{\partial s}{\partial \tau} + \frac{\partial \hat{u}}{\partial s}\frac{\partial^2 s}{\partial \tau^2} + \frac{\partial^2 \hat{u}}{\partial t^2},$$

with

$$\frac{\partial s}{\partial x} = \frac{\gamma(\tau)-\sigma_1}{d-\sigma_1}, \quad \frac{\partial s}{\partial \tau} = \frac{a(\tau)}{d-\sigma_1}x, \quad \text{in } \Omega_1^-,$$
$$\frac{\partial s}{\partial x} = 1, \qquad \frac{\partial s}{\partial \tau} = a(\tau), \qquad \text{in } \Omega_2^-.$$

Using the argument in [5, Appendix] and the differential equation $\hat{u}_t = \hat{f} + \varepsilon \hat{u}_{ss} - \hat{a}(t)\hat{u}_s$, one can deduce

$$\big\|\frac{\partial^{i+j}\hat{u}}{\partial s^i \partial t^j}\big\|_{\bar{Q}} \le C\varepsilon^{-1/2}\varepsilon^{-n},\ n = i+2j \le 4, \quad \big\|\frac{\partial^2 \hat{u}}{\partial s \partial t}\big\|_{\bar{Q}} + \big\|\frac{\partial^2 \hat{u}}{\partial t^2}\big\|_{\bar{Q}} \le C\varepsilon^{-1/2}\varepsilon^{-2}.$$

Together these yield

$$\big\|\frac{\partial^i u}{\partial x^i}\big\|_{\bar{\Omega}_1^-} \le C\varepsilon^{-1/2}(d\varepsilon)^{-i},\ \big\|\frac{\partial^i u}{\partial x^i}\big\|_{\bar{\Omega}_2^-} \le C\varepsilon^{-1/2}\varepsilon^{-i}, \quad i \le 4, \tag{15a}$$

$$\big\|\frac{\partial^2 u}{\partial \tau^2}\big\|_{\bar{\Omega}^-} \le C\varepsilon^{-1/2}\varepsilon^{-2}. \tag{15b}$$

We now recall from [5] the decomposition of the solution in the subdomain Ω^+. There is the regular component v^+, a boundary layer component w associated with $x = 1$ and an interior layer component z^+ associated with the interior layer structure to the left of Γ^*.

Lemma 3. [5] *In the region Ω^+, the solution of problem (14) can be decomposed into the sum $u = v^+ + w + z^+$ where*

$$\begin{aligned} |w(x,\tau)| &\le Ce^{-\frac{\alpha\delta}{\varepsilon}\int_{s=x}^1 \frac{s-d}{1-d}\,ds} e^{\frac{\alpha\tau}{(1-d)\delta}}, (x,\tau) \in \Omega^+, \\ \Big|\frac{\partial^j w}{\partial x^j}(x,\tau)\Big| &\le C\varepsilon^{-j}e^{-\frac{\alpha\delta(1-x)}{2\varepsilon}},\ 1 \le j \le 4,\ (x,\tau) \in \Omega^+, \\ \Big|\frac{\partial^m w}{\partial \tau^m}(x,\tau)\Big| &\le C\varepsilon^{1-m},\ (x,\tau) \in \Omega^+, \quad m = 1,2; \end{aligned}$$

with $\delta := \frac{1-\gamma(T)}{1-d} > 0$. Furthermore, it holds

$$|z^+(x,\tau)| \le Ce^{-C^*\sqrt{\frac{\alpha}{\varepsilon}}(x-d)}, \quad (x,\tau) \in \Omega^+; \quad C^* := \exp\big(\frac{\|a\|}{\delta(1-d)}T\big) \tag{16a}$$

and if $d \le x < d + (1-\gamma(T))$ and $0 \le \tau \le T$, then its partial derivatives satisfy

$$\Big|\frac{\partial^j z^+}{\partial x^j}(x,\tau)\Big| \le C\varepsilon^{-j/2},\ 1 \le j \le 4, \quad \Big|\frac{\partial^m z^+}{\partial \tau^m}(x,\tau)\Big| \le C,\ m = 1,2. \tag{16b}$$

3. Discrete problem

We approximate the solution of problem (14) on a rectangular grid in the computational domain $\bar{\Omega}$, which concentrates mesh points in the interior and boundary layers. In the original domain $\bar{Q}$ the corresponding grid is strongly time dependent because it is designed to align itself with the characteristic curve Γ^*. In Figure 1 we display the grid in the subregion $\bar{Q}^-$. The grid points of the computational domain are given by

$$\overline{\Omega}^{N,M} := \{x_i\}_{i=0}^N \times \{\tau_j\}_{j=0}^M, \tag{17a}$$

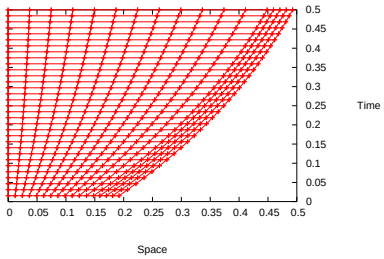

FIGURE 1. Grid in the subregion $\bar{Q}^-$.

where N and M are two positive integers. The local spatial mesh sizes are denoted by $h_i = x_i - x_{i-1}$, $1 \le i \le N$. The mesh is uniform in the time direction; so $\tau_j = jT/M$, $0 \le j \le M$. The grid points for the space variable are distributed by means of a piecewise uniform Shishkin mesh. This is defined with respect to the transition points

$$\sigma_1 = \min\{\frac{d}{4}, \sqrt{\frac{2\varepsilon}{\alpha}} \ln N\}, \tag{17b}$$

$$\sigma_2 = \min\{1-\gamma(T), C^* \sqrt{\frac{2\varepsilon}{\alpha}} \ln N\}, \tag{17c}$$

$$\sigma = \min\{\frac{1-(d+\sigma_2)}{2}, \frac{4\varepsilon}{\alpha\delta} \ln N\}, \quad C^* := \exp\big(\frac{\|a\|}{\delta(1-d)} T\big), \tag{17d}$$

which split the interval $[0,1]$ into the five subdomains

$$[0, d-\sigma_1] \cup [d-\sigma_1, d] \cup [d, d+\sigma_2] \cup [d+\sigma_2, 1-\sigma] \cup [1-\sigma, 1]. \tag{17e}$$

The grid points are uniformly distributed within each subinterval such that

$$x_0 = 0,\ x_{3N/8} = d - \sigma_1,\ x_{N/2} = d,\ x_{5N/8} = d + \sigma_2,\ x_{7N/8} = 1 - \sigma,\ x_N = 1.$$

We define the following subsets in the computational domain

$$\bar{\Omega}^{N,M,+} = \bar{\Omega}^{N,M} \cap \bar{\Omega}^+, \quad \bar{\Omega}_i^{N,M,-} = \bar{\Omega}^{N,M} \cap \bar{\Omega}_i^-, i = 1, 2.$$

We discretize problem (14) using an Euler method to approximate the time variable and an upwind finite difference operator to approximate in space. Hence the discrete problem is: Find U such that

$$(-\varepsilon g^2 \delta_x^2 + \kappa D_x^- + D_\tau^-)U = f(x_i, \tau_j),\ x_i \ne 0,\ d-\sigma_1, d, 1,\ \tau_j > 0, \tag{18a}$$

$$-\varepsilon[gD_x]U = 0,\ x_i = d - \sigma_1, d,\ \tau_j > 0, \tag{18b}$$

$$U = u(x_i, \tau_j), \quad (x_i, \tau_j) \in \partial\Omega^{N,M}; \tag{18c}$$

where we use the following notation for the finite difference operators

$$\begin{aligned}
D_x^-\Upsilon(x_i,\tau_j) &:= (\Upsilon(x_i,\tau_j)-\Upsilon(x_{i-1},\tau_j))/h_i,\ D_x^+\Upsilon(x_i,\tau_j) := D_x^-\Upsilon(x_{i+1},\tau_j),\\
[gD_x]\Upsilon(x_i,\tau_j) &:= g(x_i^+,\tau_j)D_x^+\Upsilon(x_i,\tau_j) - g(x_i^-,\tau_j)D_x^-\Upsilon(x_i,\tau_j),\\
D_t^-\Upsilon(x_i,\tau_j) &:= \frac{\Upsilon(x_i,\tau_j)-\Upsilon(x_i,\tau_{j-1})}{\tau_j-\tau_{j-1}},\\
\delta_x^2\Upsilon(x_i,\tau_j) &:= \frac{2}{h_i+h_{i+1}}(D_x^+\Upsilon(x_i,\tau_j) - D_x^-\Upsilon(x_i,\tau_j)).
\end{aligned}$$

Associated with this discrete problem is the finite difference operator

$$L^{N,M}Z(x_i,\tau_j) := \begin{cases} (-\varepsilon g^2\delta_x^2 + \kappa D_x^- + D_\tau^-)Z(x_i,\tau_j), & x_i \neq 0, d-\sigma_1, d, 1,\ \tau_j > 0,\\ -\varepsilon[gD_x]Z(x_i,\tau_j), & x_i = d-\sigma_1, d,\ \tau_j > 0,\\ Z(x_i,\tau_j), & (x_i,\tau_j)\in\partial\Omega^{N,M}. \end{cases}$$

This discrete operator satisfies a discrete comparison principle and we can then establish that

$$\|U\|_{\bar\Omega^{N,M}} \leq C.$$

4. Error Analysis

The argument in this section divides the parameter space $\{(\varepsilon,N)\,|\,0<\varepsilon\leq 1, N\geq 8\}$ into two subregions. In the first region where $N >> \varepsilon^{-1}$, then there exists some C_q such that

$$\varepsilon^{-1} \leq C_q(\ln N)^q, \quad q\geq 1. \tag{19}$$

In this case, either $\sigma = \frac{1-(d+\sigma_2)}{2}, (q=1)$, or $\sigma_2 = 1-\gamma(T), (q=2)$ or $\sigma_1 = d/4, (q = 2/(1-2p))$. For the remaining subregion of the parameter space, we assume that

$$\sigma_1 = \sqrt{\frac{2\varepsilon}{\alpha}}\ln N, \quad \sigma_2 = e^{C^*T}\sqrt{\frac{2\varepsilon}{\alpha}}\ln N, \quad \sigma = \frac{4\varepsilon}{\alpha\delta}\ln N. \tag{20}$$

Throughout most of this section, we will be dealing with the case of (20). We begin by dealing with the other case. In the case of the fine mesh transition parameter σ_1, and for any fixed N, we note that the range of values of the singular perturbation parameter ε for which the constraint (19) is satisfied increases as $p\to 0.5^-$.

At the interfaces, one can estimate the truncation errors using

$$|[gD_x](U-u)| = |[gD_xu] - [gu_x]|.$$

Then from standard truncation error bounds and the bounds (15), one can deduce the following error bounds in the case of (19)

$$|L^{N,M}(U-u)(x_i,\tau_j)| \leq C\varepsilon^{-2.5}\begin{cases} (d^{-2}N^{-1}+M^{-1}), & x_i < d-\sigma_1,\\ \varepsilon(dN)^{-1}, & x_i = d-\sigma_1, d,\\ (N^{-1}+M^{-1}), & d-\sigma_1 < x_i < d, x_i > d. \end{cases}$$

Since $d=\varepsilon^p$, it follows that

$$|U-u| \leq C\varepsilon^{-2.5}d^{-2}(N^{-1}+M^{-1}) \leq C(N^{-1}+M^{-1})(\ln N)^{\frac{5+4p}{1-2p}}.$$

In the case of (20), we consider a decomposition of the numerical solution

$$U^- = V^- + Z^-, \text{ in } \bar\Omega^{N,M,-}, \quad U^+ = V^+ + W + Z^+, \text{ in } \bar\Omega^{N,M,+}.$$

The five components are defined as the solutions of the following discrete problems:

$$\begin{aligned}
&L^{N,M}V^\pm = f, \quad \text{in } \Omega^{N,M,\pm}, \quad V^\pm = v^\pm, \quad \text{on } \partial\Omega^{N,M,\pm},\\
&L^{N,M}W = 0, \quad \text{in } \Omega^{N,M,+}, \quad W = w, \quad \text{at } x = d, 1, \quad W = 0, \text{ at } \tau = 0,\\
&L^{N,M}Z^\pm = 0, \quad \text{in } \Omega^{N,M,\pm},
\end{aligned}$$

with the initial and boundary values for the discrete interior layer component taken to be

$$Z^-(0,\tau_j) = Z^+(1,\tau_j) = 0, \quad \tau_j \in [0,T],$$
$$Z^-(x_i,0) = 0, \quad x_i \in [0,d], Z^+(x_i,0) = (U-V^+)(x_i,0), \quad x_i \in [d,1],$$
$$Z^-(d,\tau_j) = (U-V^-)(d,\tau_j), \quad Z^+(d,\tau_j) = (U-V^+-W)(d,\tau_j).$$

From [5], we assume that the discretization parameters M and N satisfy

$$M > (\ln N)\frac{(\|\hat{a}\|_{\bar{Q}} + 1 - d)T}{(1-d)\delta^2}. \tag{21}$$

In passing, we observe that although (21) is not a severe restriction on the time step, it appears from [5, Table 2] to be a necessary constraint in practice. Error estimates of the components within $\bar{\Omega}^{N,M,+}$ were established in [5]. They will be required in the error analysis of the numerical method (18).

Lemma 4. [5] *Assume (20). For M sufficiently large so that (21) is satisfied, it holds*

$$\|V^+ - v^+\|_{\bar{\Omega}^{N,M,+}} \leq CN^{-1} + CM^{-1},$$
$$\|W - w\|_{\bar{\Omega}^{N,M,+}} \leq C(N^{-1}\ln N + M^{-1})\ln N,$$
$$|(Z^+ - z^+)(x_i,\tau_j)| \leq CN^{-1}\ln N, \quad 0 \leq \tau_j \leq T,\ d+\sigma_2 \leq x_i \leq 1.$$

Now we obtain bounds for the error associated with the subdomain $\bar{\Omega}^-$. We begin with the regular component

Lemma 5. *Assume (20). It holds*

$$\|V^- - v^-\|_{\bar{\Omega}^{N,M,-}} \leq CN^{-1} + CM^{-1}. \tag{22}$$

Proof. The argument is again based on a stability and truncation error argument. For $x_i \neq d - \sigma_1$ we have

$$|L^{N,M}(V^- - v^-)(x_i,\tau_j)| \leq \begin{cases} C(N^{-1}+M^{-1}), & (x_i,\tau_j) \in \Omega_1^{N,M,-}, \\ C(N^{-1}\sqrt{\varepsilon}\ln N + M^{-1}), & (x_i,\tau_j) \in \Omega_2^{N,M,-}. \end{cases}$$

and for $x_i = d - \sigma_1$, we have

$$\varepsilon\Big|[gD_x(V^- - v^-)](x_i,\tau_j)\Big| \leq CN^{-1}\varepsilon.$$

Use the barrier function $\Phi_1(x_i,\tau_j) = C\tau(N^{-1}+M^{-1}) + CN^{-1}B_1(x_i)$, with

$$B_1(x_i) = \begin{cases} 1, & 0 < x_i < d-\sigma_1, \\ \dfrac{d-x_i}{\sigma_1}, & d-\sigma_1 \leq x_i < d, \end{cases} \tag{23}$$

to prove the result. □

Lemma 6. *Assume (20) and (21) hold, then in $\bar{\Omega}_1^{N,M,-}$ we have that,*

$$|(Z^- - z^-)(x_i,\tau_j)| \leq CN^{-1}\ln N.$$

Proof. Using the triangular inequality and Lemma 2, we have

$$|(Z^- - z^-)(x_i,\tau_j)| \leq CN^{-1} + |Z^-(x_i,\tau_j)|.$$

Now, we deduce appropriate bounds for the discrete function $Z^-(x,\tau)$ in $\bar{\Omega}_1^{N,M,-}$. We define the following discrete barrier function

$$\Phi_2(x_i,\tau_j) := C(1 - \frac{\alpha T}{\delta^2 M})^{-j}\Big(B_2(x_i) + B_2(x_{3N/8})B_1(x_i)\ln N\Big),$$

where

$$B_2(x_i) = \frac{\Pi_{k=1}^{i}\left(1+\frac{\sqrt{\alpha}h_k}{\sqrt{2\varepsilon}}\right)}{\Pi_{k=1}^{N/2}\left(1+\frac{\sqrt{\alpha}h_k}{\sqrt{2\varepsilon}}\right)},$$

and the function $B_1(x)$ is given in (23). It is a modification of the discrete barrier function given in [5], which allows one establish the inequality

$$-[gD_x\Phi_2](d-\sigma_1,\tau_j) \geq 0.$$

Noting that $\Phi_2(x_i,\tau_j) \geq CN^{-1}\ln N$, if $x_i \leq d-\sigma_1$; the result follows. □

The next theorem presents a result of global convergence in the domain $\bar{Q}$. We use the notation $\hat{U}(s,t) = U(x,\tau)$, where U is the solution of (18) in the computational domain $\bar{\Omega}^{N,M}$.

Theorem 1. *Assume (21) holds. For $p < 1/2$,*

$$\begin{aligned}
\|(\bar{\hat{U}}-\hat{u})(s,t)\|_{\bar{Q}} &\leq C(N^{-1}+M^{-1})(\ln N)^{\frac{5+4p}{1-2p}}, \quad \text{in the case of (19)},\\
\|(\bar{\hat{U}}-\hat{u})(s,t)\|_{\bar{Q}} &\leq C(N^{-1}\ln N+M^{-1})\ln N, \quad \text{in the case of (20)};
\end{aligned}$$

where $\hat{u}$ is the solution of (1), (3) and $\bar{\hat{U}}$ is the linear interpolant of $\hat{U}$ in the domain $\bar{Q}$.

Proof. We only need to consider the case of (20). We first establish the error bound at the mesh points. Consider the region $\bar{R}^{N,M} = \bar{\Omega}^{N,M} \cap \{[d-\sigma_1, d+\sigma_2]\times[0,T]\}$. From the previous lemmas, it trivially holds this result in $\bar{\Omega}^{N,M}\backslash R^{N,M}$. In the region $R^{N,M}$ for $x_i \neq d$, it holds

$$|L^{N,M}(U-u)(x_i,\tau_j)| \leq \begin{cases} CN^{-2}\ln^2 N + CM^{-1}, & d-\sigma_1 < x_i < d,\\ CN^{-1}\ln^2 N + CM^{-1}, & d < x_i < d+\sigma_2. \end{cases}$$

At $x_i = d$, note that

$$\begin{aligned}
|u_x(d^-,\tau_j) - D_x^- u(d,\tau_j)| &\leq |v_x^-(d^-,\tau_j) - D_x^- v^-(d,\tau_j)|\\
&\quad + |z_x^-(d^-,\tau_j) - D_x^- z^-(d,\tau_j)| \leq CN^{-1}\sigma_1 + C\tfrac{N^{-1}\sigma_1}{\varepsilon},
\end{aligned}$$

with a similar bound to the right of d. Hence,

$$\varepsilon|[gD_x(U-u)](d,\tau_j)| \leq CN^{-1}\ln N\sqrt{\varepsilon}.$$

To obtain the error bound nodally, use the barrier function

$$\Phi_3(x_i,\tau_j) = C(N^{-1}\ln N + M^{-1})\ln N(\tau+1) + CN^{-1}(\ln N)^2 B_3(x_i),$$

where B_3 is a piecewise linear function defined by $B_3(d-\sigma_1) = B_3(d+\sigma_2) = 0$, $B_3(d) = 1$. Use the argument in [5, Theorem 9] to complete the proof. □

5. Numerical experiments

The theory in this paper is restricted to the case where the point $(d,0)$, which is the location of the interior layer in the initial condition, is bounded away from the inflow corner $(0,0)$ by a distance strictly greater than $C\sqrt{\varepsilon}$. Below, in §5.1, we present numerical results which support this theory. In addition, in §5.2, we present some numerical results for the case when $0 < d \leq C\sqrt{\varepsilon}$, for which we have no corresponding theory.

5.1. The case when $C\sqrt{\varepsilon} < d = \varepsilon^p < 1$. Consider the following test problem

$$-\varepsilon \hat{u}_{ss} + e^{-2t}\hat{u}_s + \hat{u}_t = 4s(1-s)e^t, \quad (s,t) \in (0,1)\times(0,0.5], \tag{24a}$$

$$\hat{u}(s,0) = \hat{\phi}(s;\varepsilon,d), \quad 0 \le s \le 1, \tag{24b}$$

$$\hat{u}(0,t) = 2t^3, \ \hat{u}(1,t) = 1, \ 0 < t \le 0.5, \tag{24c}$$

and the initial condition $\hat{\phi}$ is given by

$$\hat{\phi}(s;\varepsilon,d) = \begin{cases} 0, & \text{if } 0 \le s \le d, \\ (1 - e^{-\frac{(1-d)}{\sqrt{\varepsilon}}})^{-4}(1 - e^{-\frac{(s-d)}{\sqrt{\varepsilon}}})^4, & \text{if } d < s \le 1. \end{cases} \tag{24d}$$

In Figure 2 we display the numerical approximation of the solution of problem (24) for $\varepsilon = 2^{-20}$, $d = \varepsilon^{1/4}$, and $N = M = 32$. From this figure we observe that the solution exhibits an interior layer emanating close to the corner $(0,0)$, which is clearly visible in the figure, and also a boundary layer at the edge $x = 1$. Note also that the Shishkin mesh (17a) locates grid points in both the interior and boundary layers.

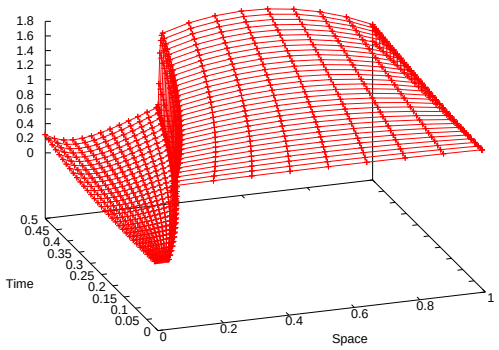

FIGURE 2. Numerical approximation of the solution of problem (24) for $\varepsilon = 2^{-20}$, $d = \varepsilon^{1/4}$, and $N = M = 32$.

The exact solution of problem (24) is unknown. We estimate the global pointwise errors using the double mesh principle [3] to compute the global two–mesh differences $\bar{D}_\varepsilon^N$ for each value of $\varepsilon \in S_\varepsilon = \{2^{-6}, 2^{-9}, \ldots, 2^{-40}\}$, and the uniform global differences $\bar{D}^N$:

$$\bar{D}_\varepsilon^N := \left\| \bar{\hat{U}}^{N,N} - \bar{\hat{U}}^{2N,2N} \right\|_{\bar{Q}^{N,N}}, \ \bar{D}^N := \max_{\varepsilon \in S_\varepsilon} \bar{D}_\varepsilon^N,$$

where a numerical approximation $U^{2N,2N}$ is computed on a finer mesh $\bar{\Omega}^{2N,2N}$ and $\bar{Q}^{N,N} := \{(s_i^j, t_j)\} \subseteq \bar{Q}$ with

$$(x_i, \tau_j) = X(s_i^j, t_j), \quad (x_i, \tau_j) \in \bar{\Omega}^{N,N} \cup \bar{\Omega}^{2N,2N}.$$

Hence, we have

$$s_i^j := \begin{cases} x_i + \gamma(\tau_j) - d, & \text{if } x_i \in \Omega_2^-, \\ \dfrac{\gamma(\tau_j) - \sigma_1}{d - \sigma_1} x_i, & \text{if } x_i \in \Omega_1^-, \\ 1 - \dfrac{1 - \gamma(\tau_j)}{1 - d}(1 - x_i), & \text{if } x_i \in \Omega^+. \end{cases}$$

The interpolation is taken over the domain $\bar{Q}$, i.e., for each $t := t_j$, and $s_i^j \le s \le s_{i+1}^j$

$$\bar{\hat{U}}^{N,N}(s,t_j) := \hat{U}^{N,N}(s_{i+1}^j,t_j)\frac{s-s_i^j}{s_{i+1}^j-s_i^j} + \hat{U}^{N,N}(s_i^j,t_j)\frac{s_{i+1}^j-s}{s_{i+1}^j-s_i^j}.$$

From these values we calculate computed orders of global convergence $\bar{P}_\varepsilon^N$ and computed orders of global uniform convergence $\bar{P}^N$ using

$$\bar{P}_\varepsilon^N := \log_2\left(\frac{\bar{D}_\varepsilon^N}{\bar{D}_\varepsilon^{2N}}\right),\ \bar{P}^N := \log_2\left(\frac{\bar{D}^N}{\bar{D}^{2N}}\right).$$

In Table 1 we display the global differences and uniform global differences for problem (24) with their corresponding orders of global convergence for $d = \varepsilon^{1/4}$. Note that the method converges for all the values of $\varepsilon \in S_\varepsilon$. Over the range of ε and N considered, the largest global difference was seen to be located within the interior layer. The noticeable drop in the orders of convergence in Table 1 between $N = 256$ and $N = 512$ coincides with a shift in the location for the largest global difference. For $N \le 256$ the largest difference was observed to occur near the initial time $t = 0$ and for $N \ge 512$ the location abruptly moved, being close to $t = T/2$ for $N = 512$ and at the final time $t = T$ for $N \ge 1024$. The uniform orders of global convergence indicate that the method is almost first order uniformly convergent and suggest that the exponent of $\ln N$ given in the asymptotic error bound in Theorem 1 may be somewhat pessimistic.

5.2. The case when $0 < d \le C\sqrt{\varepsilon}$. In the case of $d \le C\sqrt{\varepsilon}$, we re-consider the method analysed in [5]. This method involves a single coordinate transformation and was analysed only for the case of d independent of ε. However, the method given in [5] is still applicable when $d \le C\sqrt{\varepsilon}$. In fact, one can establish a parameter-uniform error estimate of the form

$$|(\hat{U}-\hat{u})(s_i,t_j)| \le CN^{-1}(\ln N), \quad (s_i,t_j) \in \bar{Q}^*,$$

where

$$\bar{Q}^* := \bar{Q} \setminus \{(s,t)\,|\,\gamma(t) - C\sqrt{\varepsilon}\ln N \le s \le \gamma(t) + C\sqrt{\varepsilon}\ln N,\ t > 0\}.$$

This bound gives no information about the numerical error within the internal layer. The main obstacle to obtaining a bound, indicating parameter-uniform convergence within the layer, resides in the inability to apply the classical interior *a priori* bounds on the derivatives of the solution in the vicinity of the corner region $\{(s,t)\,|\,s \le C\sqrt{\varepsilon},\ t \le \delta = O(1)\}$. In Table 2, global two-mesh differences are presented which suggest that the numerical method is globally accurate throughout the entire domain. A representative computed solution is displayed in Figure 3.

Acknowledgments

This research was partially supported by the project MEC/FEDER MTM 2010-16917 and the Diputación General de Aragón.

References

[1] A. Friedman, *Partial differential equations of parabolic type*, Prentice-Hall, Englewood Cliffs, N.J., (1964).

[2] O.A. Ladyzhenskaya, V.A. Solonnikov and N.N. Ural'tseva, *Linear and quasilinear equations of parabolic type*, Transactions of Mathematical Monographs, **23**, American Mathematical Society, (1968).

[3] P.A. Farrell, A.F. Hegarty, J.J.H. Miller, E. O'Riordan and G.I. Shishkin, *Robust Computational Techniques for Boundary Layers*, Chapman and Hall/CRC Press, Boca Raton, U.S.A., (2000).

TABLE 1. Two–mesh global differences, uniform global differences and the computed orders of global convergence for test problem (24) with $d = \varepsilon^{1/4}$.

	N=64 M=64	N=128 M=128	N=256 M=256	N=512 M=512	N=1024 M=1024	N=2048 M=2048
$\varepsilon = 2^{-6}$	0.709E-02 1.158	0.318E-02 1.053	0.153E-02 1.029	0.751E-03 1.015	0.371E-03 1.008	0.185E-03 1.004
$\varepsilon = 2^{-8}$	0.483E-01 1.552	0.165E-01 0.961	0.846E-02 0.986	0.427E-02 0.995	0.214E-02 0.998	0.107E-02 0.999
$\varepsilon = 2^{-10}$	0.144E+00 1.147	0.650E-01 1.976	0.165E-01 0.979	0.838E-02 0.994	0.421E-02 0.999	0.210E-02 1.000
$\varepsilon = 2^{-12}$	0.596E-01 -1.033	0.122E+00 1.032	**0.597E-01** 1.865	**0.164E-01** 0.963	**0.840E-02** 0.999	**0.420E-02** 1.001
$\varepsilon = 2^{-14}$	0.791E-01 -0.629	0.122E+00 1.169	0.544E-01 2.004	0.136E-01 0.837	0.759E-02 0.852	0.420E-02 0.864
$\varepsilon = 2^{-16}$	0.964E-01 -0.377	0.125E+00 1.270	0.519E-01 2.021	0.128E-01 0.845	0.712E-02 0.855	0.394E-02 0.862
$\varepsilon = 2^{-18}$	0.117E+00 -0.152	0.130E+00 1.341	0.515E-01 2.068	0.123E-01 0.847	0.683E-02 0.855	0.378E-02 0.865
$\varepsilon = 2^{-20}$	0.141E+00 0.031	0.138E+00 1.396	0.525E-01 2.135	0.119E-01 0.848	0.664E-02 0.853	0.367E-02 0.869
$\varepsilon = 2^{-22}$	0.156E+00 0.077	**0.148E+00** 1.440	0.544E-01 2.131	0.124E-01 0.934	0.651E-02 0.852	0.360E-02 0.871
$\varepsilon = 2^{-24}$	0.158E+00 0.104	0.147E+00 1.417	0.549E-01 2.096	0.128E-01 1.002	0.641E-02 0.851	0.356E-02 0.872
$\varepsilon = 2^{-26}$	0.159E+00 0.122	0.146E+00 1.426	0.543E-01 2.092	0.127E-01 1.005	0.635E-02 0.851	0.352E-02 0.873
$\varepsilon = 2^{-28}$	0.160E+00 0.135	0.146E+00 1.432	0.539E-01 2.087	0.127E-01 1.009	0.631E-02 0.850	0.350E-02 0.874
$\varepsilon = 2^{-30}$	0.160E+00 0.144	0.145E+00 1.437	0.536E-01 2.084	0.127E-01 1.012	0.627E-02 0.850	0.348E-02 0.874
$\varepsilon = 2^{-32}$	0.161E+00 0.150	0.145E+00 1.440	0.534E-01 2.081	0.126E-01 1.014	0.625E-02 0.850	0.347E-02 0.874
$\varepsilon = 2^{-34}$	0.161E+00 0.154	0.145E+00 1.442	0.533E-01 2.079	0.126E-01 1.016	0.624E-02 0.850	0.346E-02 0.874
$\varepsilon = 2^{-36}$	0.161E+00 0.157	0.145E+00 1.443	0.532E-01 2.078	0.126E-01 1.017	0.623E-02 0.849	0.346E-02 0.874
$\varepsilon = 2^{-38}$	0.161E+00 0.159	0.145E+00 1.444	0.531E-01 2.077	0.126E-01 1.017	0.622E-02 0.849	0.345E-02 0.874
$\varepsilon = 2^{-40}$	**0.162E+00** 0.161	0.144E+00 1.445	0.531E-01 2.077	0.126E-01 1.018	0.621E-02 0.849	0.345E-02 0.874
$\bar{D}^N$ $\bar{P}^N$	0.162E+00 0.129	0.148E+00 1.308	0.597E-01 1.865	0.164E-01 0.963	0.840E-02 0.936	0.420E-02 1.001

[4] F.J. Gaspar, F.J. Lisbona and P.N. Vabishchevich, *A finite difference analysis of Biot's consolidation model*, Appl. Numer. Math., **44**, 2003, 487–506.
[5] J.L. Gracia and E. O'Riordan, A singularly perturbed convection–diffusion problem with a moving interior layer, *Inter. J. Numer. Anal. Mod.*, **9**, 2012, 823–843.
[6] G.I. Shishkin, Limitations of adaptive mesh refinememt techniques for singularly perturbed problems with a moving interior layer, *J. Comp. Appl. Math.*, **166**, 2004, 267–280.

Department of Applied Mathematics, University of Zaragoza, Spain.
E-mail: jlgracia@unizar.es

School of Mathematical Sciences, Dublin City University, Dublin 9, Ireland.
E-mail: eugene.oriordan@dcu.ie

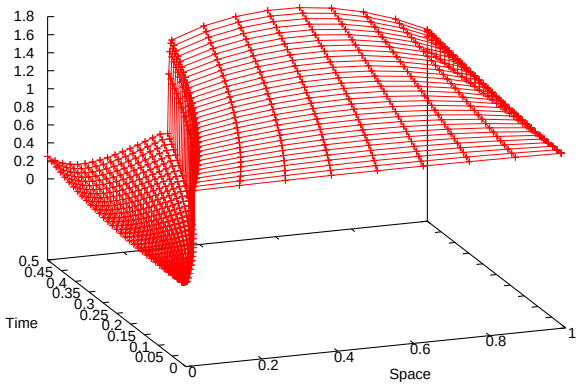

FIGURE 3. Numerical approximation of the solution of problem (24) for $\varepsilon = 2^{-20}$, $d = \varepsilon$, and $N = M = 32$ using the numerical method from [5].

TABLE 2. Two–mesh global differences, uniform global differences, and the computed orders of convergence for the numerical method given in [5] applied to the test problem (24) with $d = \varepsilon$.

	N=64 M=64	N=128 M=128	N=256 M=256	N=512 M=512	N=1024 M=1024	N=2048 M=2048
$\varepsilon = 2^{-6}$	0.252E-01 1.012	0.125E-01 1.011	0.621E-02 1.007	0.309E-02 1.004	0.154E-02 1.002	0.770E-03 1.001
$\varepsilon = 2^{-7}$	0.510E-01 1.597	0.169E-01 1.035	0.823E-02 1.022	0.405E-02 1.013	0.201E-02 1.007	0.100E-02 1.004
$\varepsilon = 2^{-8}$	0.927E-01 2.006	0.231E-01 1.124	0.106E-01 1.024	0.521E-02 1.014	0.258E-02 1.008	0.128E-02 1.004
$\varepsilon = 2^{-9}$	**0.119E+00** 1.201	0.518E-01 1.884	0.140E-01 1.017	0.694E-02 1.015	0.343E-02 1.010	0.171E-02 1.005
$\varepsilon = 2^{-10}$	0.799E-01 -0.225	0.933E-01 2.014	0.231E-01 1.287	0.947E-02 1.013	0.469E-02 1.011	0.233E-02 1.007
$\varepsilon = 2^{-11}$	0.661E-01 -0.539	0.960E-01 1.324	**0.384E-01** 1.540	**0.132E-01** 1.016	**0.652E-02** 1.013	0.323E-02 1.008
$\varepsilon = 2^{-12}$	0.663E-01 -0.535	**0.961E-01** 1.332	0.382E-01 1.729	0.115E-01 0.870	0.629E-02 0.853	**0.349E-02** 0.875
$\varepsilon = 2^{-13}$	0.664E-01 -0.532	0.961E-01 1.336	0.381E-01 1.726	0.115E-01 0.877	0.627E-02 0.852	0.347E-02 0.875
$\varepsilon = 2^{-14}$	0.665E-01 -0.531	0.961E-01 1.336	0.381E-01 1.726	0.115E-01 0.881	0.625E-02 0.852	0.346E-02 0.875
$\varepsilon = 2^{-15}$	0.666E-01 -0.529	0.961E-01 1.336	0.381E-01 1.726	0.115E-01 0.883	0.624E-02 0.852	0.346E-02 0.875
. . .	. . .	. . .	. . .	. . .	. . .	. . .
$\varepsilon = 2^{-40}$	0.667E-01 -0.527	0.961E-01 1.336	0.381E-01 1.727	0.115E-01 0.888	0.622E-02 0.852	0.345E-02 0.874
$\bar{D}^N$ $\bar{P}^N$	0.119E+00 0.309	0.961E-01 1.326	0.384E-01 1.540	0.132E-01 1.016	0.652E-02 0.904	0.349E-02 0.875